



# Incendios Forestales: amenazas y oportunidades ante los desafíos de un entorno cambiante

Comunicaciones científico-profesionales

X SIMPOSIO NACIONAL SOBRE INCENDIOS FORESTALES  
**ESPAÑA**

## FOREST FUEL MANAGEMENT IN WILDLAND URBAN INTERFACE AREAS

Authors: Ribeiro, C.<sup>1\*</sup>, Xavier Viegas, D.<sup>1,2</sup>, Almeida, M.<sup>1</sup>, Ribeiro, L.<sup>1</sup>, Rodrigues, A.<sup>1</sup>, Raposo, J.<sup>1</sup> and, Alves, D.<sup>1</sup>

<sup>1</sup> ADAI/LAETA, University of Coimbra, Coimbra, Portugal

<sup>2</sup> Department of Mechanical Engineering, University of Coimbra, Coimbra, Portugal

\*Corresponding author: Carlos Fernando Morgado Ribeiro, [carlos.ribeiro@adai.pt](mailto:carlos.ribeiro@adai.pt)

### *Abstract:*

Every year, all around the World, wildfires devastate large areas of wildland and create multiple socioeconomic impacts, especially in fire prone regions. In countries such as Portugal, Spain, France, Italy or Greece, every year the average burned area and the number of the fires is approximately between 24k to 164k and 1.5k to 18k, respectively. In Portugal, the problem of wildfires in the last decades has been increasing over the years, with severe impacts on society. The largest forest fires occurred in Portugal, in recent years, caused the destruction of several constructions (e.g. houses and manufacturing facilities, etc). More than 500 constructions were destroyed by the wildfires of June and October 2017, at north and centre regions of Portugal. The majority of those destroyed buildings could have been saved if the constructions had a proper design and if forest fuel management in the surroundings of the constructions had been performed. In 90% of the damaged constructions, the ignition resulted from spotting, with embers being deposited in vulnerable elements (e.g. roofs, windows and other openings parts) and in forest fuel near the constructions. This work intends to explore different patterns of fuel management in Wildland Urban Interface (WUI), aiming at maximizing the cost/efficiency relation as well as their efficiency.

We present a novel methodology regarding fuel management around isolated constructions in forested and rural areas. The focus is on the wildfire's history and the topographic features around the location of constructions that need protection. With this methodology it is expected that the safety of the constructions is increased and the cost for the management of the fuels close to them decreases.

In order to support this methodology, a set of experimental study tests was carried out in the Forest Fire Research Laboratory of the University of Coimbra in Lousã (Portugal) in a specific combustion table, called dihedral table.

### **Keywords:**

Wildland-urban interface, fire risk prevention, fuel breaks, infrastructures, best practices.

## Introduction.

Wildfires cause in society a considerable socio-economic impact and high negative impacts in Mediterranean areas or in wildfire prone zones (Alcasena *et al.* 2019). According Alcasena *et al.* 2019 and Moreira *et al.* 2011, in southern Europe the yearly average of the burned areas is approximately 500k hectares and the number of the fires is approximately 50k. The main risks and the worst problems caused by large and devastating fires are the human lives losses (Costa *et al.* 2011; Cardil *et al.* 2017). The climate change during the last decades and the increasing availability of fuel load in wildland areas is one of the main causes for those types of “Large-Fires” (Barrera-Escoda 2011; Moreira *et al.* 2011; Cardil *et al.* 2014).

The largest forest fires occurred in Portugal, in recent years, caused the destruction of several buildings (e.g. houses and manufacturing facilities, etc). More than 500 constructions were destroyed by the wildfires of June and October 2017, in the north and centre regions of Portugal. The majority of those destroyed buildings could have been saved if the constructions had a proper design and if forest fuel management in the surroundings of the constructions had been performed correctly (Manzello *et al.* 2012; Viegas *et al.* 2017).

Regardless of prevention efforts at landscape level, wildfires will continue to impact on people and their assets, and they tend to be increasingly destructive, costly and socially threatening (Abrams *et al.* 2014; Valente *et al.* 2015). The number of destroyed constructions is also increasing and the future tendency is to remain growing, either due to climate change or to urban growth in Wildland Urban Interface (WUI) areas. Fuel management is very important to decrease the probability of damage to infrastructures caused by wildfires.

## Objectives.

The purpose of this work is to present a novel methodology regarding fuel management around constructions in forested and rural areas. The main focus is on the wildfire’s history and the topographic features surrounding the location of constructions that need protection. In the present study only the topographic variable will be analysed. All the presented tests were performed at ADAI’s Forest Fire Research Laboratory, in a Dihedral table with two independent test beds or surfaces that allow different combinations of slope, as shown in **Figure 1**. The tests were performed without wind and spotting is not considered.

## Materials and method.

### *Physical problem.*

The slope angles considered are described schematically in **Figure 1**. An absolute reference frame  $O_oX_oY_oZ_o$  in which the horizontal datum plane was considered and is defined by the axis  $O_oX_o$  and  $O_oY_o$ . A second reference frame is defined by OXYZ and the axis OY is parallel to  $O_oY_o$  and OZ is rotated by an angle  $\alpha$  in relation to  $O_oY_o$ . This angle ( $\alpha$ ) will be designated as slope angle.

The surfaces of the ridge table are two square planar slopes and the angles can be inclined independently. It was considered  $ACDH$  and an angle  $\alpha_l$  in face  $F_1$  and  $DEGH$

and an angle  $\alpha_2$  in face  $F_2$ , as shown in Figure 1. Let us consider, in Figure 1 a) – Case 1 – angle  $\alpha_1$  was  $30^\circ$  and the angle  $\alpha_2$  was  $0^\circ$  and in Figure 1 b) – Case 2 – angle  $\alpha_1$  was  $0^\circ$  and the angle  $\alpha_2$  was  $30^\circ$ . These two scenarios represent fire spreading upslope or downslope in relation to the structure and a different distance of the fuel management for each condition, as shown in Figure 2. A linear fire front  $AC$  or  $EG$  was ignited for the upslope and downslope fire spread, respectively, (Figure 1). Henceforth, this is designated as Line  $l_i$  and is represented as a red line in Figure 1.

At the top of the ridge a wooden house was placed, built with a scale factor of 1/16 (presented in the Methods section) compared with the common rural houses in Portugal, as shown Figure 1. Henceforth, the wooden house will be designated as infrastructure. The external faces of the infrastructure were defined as  $f_1, f_2, f_3$  and  $f_4$  and the left and right faces of the roof were defined as  $f_5$  and  $f_6$ , respectively. The external face  $f_1$  and  $f_3$  are parallel to the OY axis and to the fire front. The face  $f_1$  is totally exposed to fire front when the fire spreads upslope and the face  $f_3$  is totally exposed when the fire spreads downslope. The temperature of each outside face, roof and inside of the infrastructure were monitored with K type thermocouples in contact with the wall surface. The temperature was recorded with a frequency of 1Hz by the array of thermocouples.

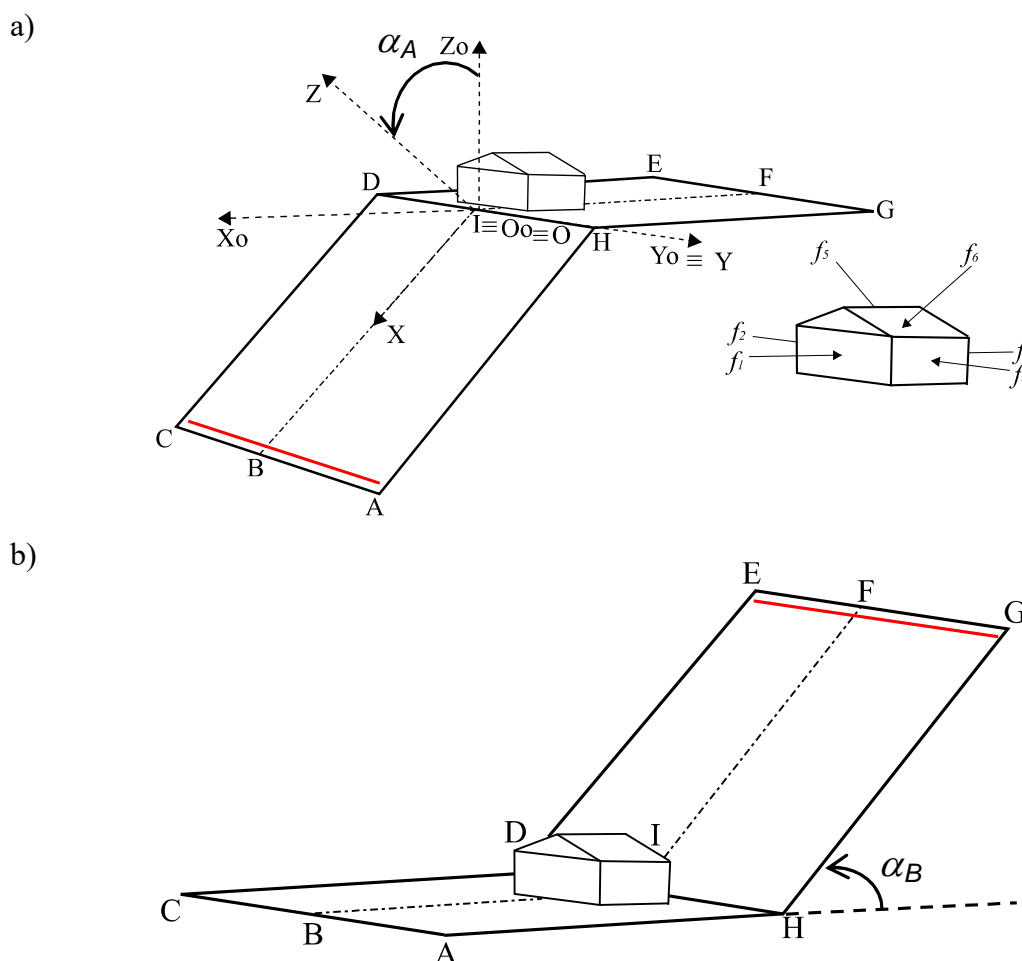


**Figure 1.** Schematic view of the test preformed: a) Case 1 - fire spreading upslope; b) Case 2 - fire spreading downslope.

The fuel management options surrounding the infrastructure are schematized in **Figure 2**. The dash line represents the top of the ridge. The infrastructure area ( $A_h$ ) is represented by the white rectangle with external red line and defined by:

$$A_h = g \times h. \tag{1}$$

Near to the external faces of the structure (grey rectangle) we considered the absence of fuel (load is equal to  $0 \text{ kg.m}^{-2}$ ), as shown in **Figure 2**. This area without fuel is important because, in this way, we ensure that there is no fuel in contact with the infrastructure. In the present study, this area ( $A_{ef}$ ) is obtained by:

$$A_{ef} = (g + b_2 + b_3) \times (h + a_2 + a_3) - A_h. \tag{2}$$

The distance around all faces of the infrastructure is constant in all directions and we considered that variables  $b_2, b_3, a_2, a_3$  has the same dimension. The fuel management area around the infrastructure is defined by the equation:

$$A_{fm} = a \times b - (A_{ef} + A_h), \tag{3}$$

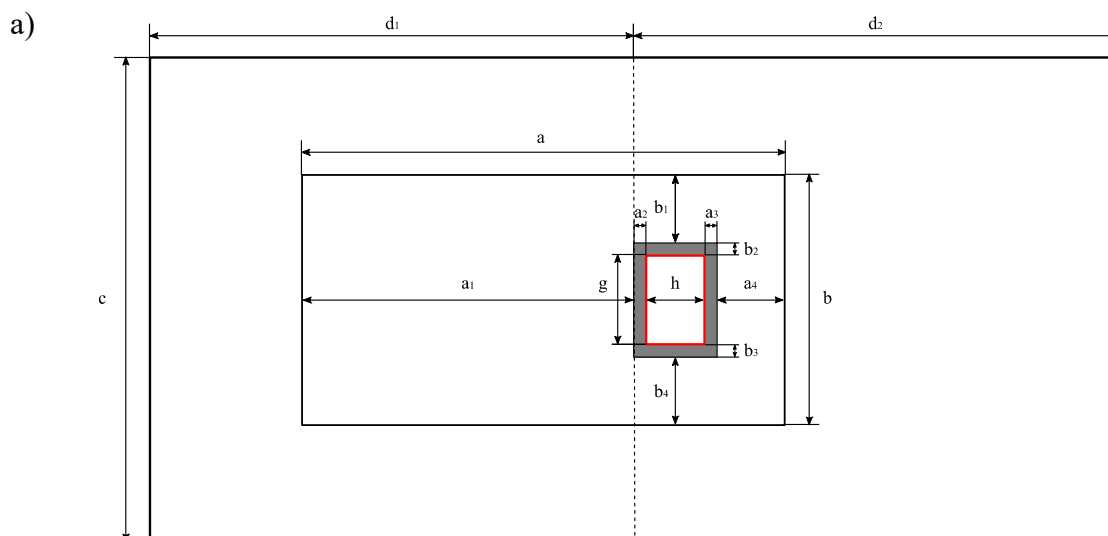
where

$$a = \sum_{i=1}^4 a_i + h \tag{4}$$

and

$$b = \sum_{i=1}^4 b_i + g. \tag{5}$$

The novel methodology presented here considers: a rectangular area for the fuel management; the house is not concentric with the fuel management area and a distance of the fuel management in the face exposed when the fire spreads upslope is larger compared with the face exposed when the fire spreads downslope or parallel with other faces.



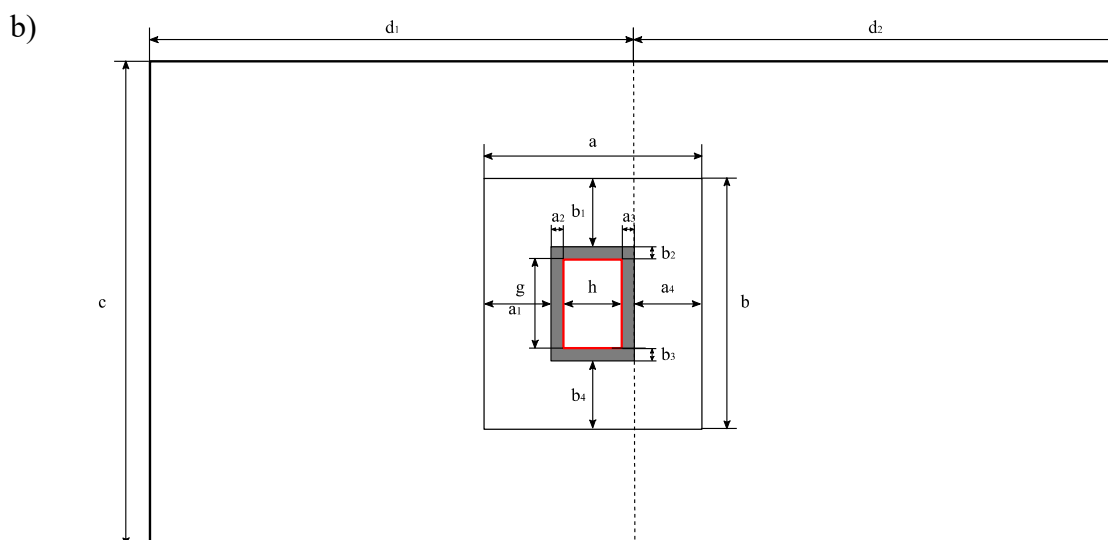


**Figure 2.** Schematic view of the fuel management around the infrastructure: a) Case 1 – test with fire spreading upslope; b) Case 2 – test with fire spreading downslope.

**Methods.**

The experimental research tests were carried out at the Forest Fire Research Laboratory of ADAI (University of Coimbra, Portugal) in Lousã on the Dihedral table. The Dihedral table has two square faces with a total test area ( $A_b$ ) defined by:

$$A_b = A_1 + A_2 \tag{6}$$

where

$$A_1 = c \times d_1, \tag{7}$$

$$A_2 = c \times d_2 \tag{8}$$

and  $c$ ,  $d_1$  and  $d_2$  measure  $4\text{ m}$ . Therefore, the  $A_1$  and  $A_2$  is equal to  $4 \times 4\text{ m}^2$  and  $A_b$  results in  $32\text{ m}^2$  test area. Each surface of the Dihedral table can be inclined independently between  $-45^\circ$  and  $+45^\circ$  in relation to the horizontal reference.

For the present study we considered a scale factor  $1/16$  that corresponds to the ratio of laboratory model to the real scale. So, in **Table 1** the corresponding values between laboratory and real scale values are presented.

	Real scale (m)		Laboratory Dimension (m)	
	Case 1	Case 2	Case 1	Case 2
$a_1$	0 / 25 / 50	12.5	0 / 1.56 / 3.125	0.781
$a_2=a_3=b_2=b_3$	3		0,186	
$a_4=b_1=b_4$	12.5	0 / 12.5	0.781	0 / 0.781
$c$	64		4	
$d_1=d_2$	64		4	
$g$	10		0.625	
$h$	7		0.438	

**Table 1.** Scale factor between real scale and laboratory dimensions.

The fuel bed was made with straw with a fuel load of  $0.6 \text{ kg.m}^{-2}$  (dry basis) outside of the fuel management area ( $m_{co}$ ) and  $0$  or  $0.2 \text{ kg.m}^{-2}$  inside of the fuel management area ( $m_{ci}$ ). The red line in Figure 1 represents the fire Line  $l_i$  (as previously mentioned) and was ignited  $0.20\text{m}$  above the edge  $AC$  or  $EG$ . This distance considered for starting the ignition is related to ensuring that there is enough fuel bed to start burning and the combustion can be sustained.

During each test, the conditions of the fuel load and bulk density were controlled during the preparation, and air temperature ( $^{\circ}\text{C}$ ), relative humidity (%) and fuel moisture ( $m_f$ ) were monitored. The time between the preparation of the fuel bed and the beginning of the test did not exceed ten minutes. This was to ensure that there were no changes in the moisture content of the fuel in contact with ambient air. During the present tests the value of fuel moisture content was measured twice: during the preparation of the fuel bed and before the ignition of each test. According Byram 1959 and Pyne *et al.* 1996 the fuel moisture content determines if the forest fuels burn and what proportion of it is available for the combustion process. In Table 2 the values of the moisture content immediately before each test are shown. Moisture content was measured with a moisture analyser (A&D ML50) was used.

The tests were monitored using an infrared camera (FLIR SC660) in continuous mode to record all test in the range  $0^{\circ}\text{C}$  to  $500^{\circ}\text{C}$  or  $300^{\circ}\text{C}$  to  $1500^{\circ}\text{C}$ , with a rate of acquisition of  $15\text{Hz}$ , a photographic camera (Canon EOS 550D) and two video cameras – one in the frontal plane (Sony AVCHD MPEG2 SD) and one in the lateral plane (Sony HD DCR-SR87). In order to reduce uncertainty three replications (T1, T2 and T3) were performed for each set of parameters, shown in Table 2. The videos recorded with the infrared camera were analysed to obtain frames of the fire front at pre-defined times. The time between frames was adjusted for each test and it was used to calculate the Rate of Spread (ROS) of the fire front. The ROS ( $\text{cm.s}^{-1}$ ) is calculated by the equation:

$$R = \frac{x_2 - x_1}{t_2 - t_1} \quad (9)$$

in the present study we used the non-dimensional ROS calculated by:

$$R' = \frac{R}{R_o}, \quad (10)$$

where  $R_o$  represent the basic ROS ( $\text{cm.s}^{-1}$ ). More details of this methodology can be consulted in Viegas 2005.

The fire front during the burning process produces heat energy. According to Byram (1959) the fire intensity ( $I$ ) is the rate of heat energy release per unit time per unit of fire front ( $\text{kW.m}^{-1}$ ) and can be calculated by

$$I = H_c M_c R, \quad (11)$$

where  $H_c$  is the fuel low heat of combustion ( $\text{kJ.kg}^{-1}$ ),  $M_c$  is weight of fuel consumed per unit area ( $\text{kg.m}^{-2}$ ) in the active flaming zone and  $R$  is the ROS of the fire front ( $\text{m.s}^{-1}$ ). Let us consider the  $H_c$  value is  $20000 \text{ kJ.kg}^{-1}$  and the  $M_c$  values are presented in Table 2. According to Rothermel and Deeming (1980) the fire intensity and the flame geometry of the fire are directly related and thus fire intensity results in

$$I = 259,833 L^{2,174} \quad (12)$$

where  $L$  (m) represents the flame length.

The thermocouples to register the temperature ( $^{\circ}\text{C}$ ) in the wall of the infrastructures were connected to NI cDAQ-9174 with a TC module NI 9213 that allows synchronous data-logging. The temperature was registered during all the time of the test. Let us consider the next equation:

$$Q' A \partial t = C_e m \partial T \quad (13)$$

where  $Q'$  represents the flux of the heat energy ( $\text{W.m}^{-2}$ ) calculated by an heat flux sensor,  $A$  represents the face area exposed to the fire front,  $\partial$  represents a differential time (s),  $C_e$  is the specific heat of the wood ( $\text{J.kg}^{-1}.\text{^{\circ}C}^{-1}$ ),  $m$  represents weight of the exposed wall to the fire front and  $\partial T$  represents a differential temperature of the exposed wall ( $^{\circ}\text{C}$ ). The temperature gradient is the difference of the temperature per unit of time and can be calculated through the equation 11 and results in

$$\frac{\partial T}{\partial t} = \frac{Q' A}{C_e m} \quad (14)$$

Ref.	$\alpha_A$ ( $^{\circ}$ )	$\alpha_B$ ( $^{\circ}$ )	$b_1$ and $b_4$ (m)	$a_4$ (m)	$a_1$ (m)	$m_{co}$ ( $\text{kg.m}^{-2}$ )	$m_{ci}$ ( $\text{kg.m}^{-2}$ )	Designation			$m_f$ (%)			$R_o$ ( $\text{cm.s}^{-1}$ )		
								T1	T2	T3	T1	T2	T3	T1	T2	T3
1					50		0	FM01	FM04	FM07	10.9	10.13	11.73	0.78	0.80	0.73
2				12.5			0.2	FM02	FM05	FM08	10.9	10.13	11.73	0.77	0.80	0.73
3	30	0			25			FM03	FM06	FM09	10.6	10.01	10.13	0.77	0.80	0.67
4			12.5	0	0	0.6	0.6	FM10	FM11	-	10.13	11.98	-	0.83	0.83	-
5							0	FM14	-	-	10.13	-	-	0.83	-	-
6	0	30		12.5	12.5		0.2	FM15	-	-	10.13	-	-	0.83	-	-
7				0	0		0.6	FM16	-	-	10,13	-	-	0,83	-	-

**Table 2.** Data of the tests performed for different fuel loads and distances, inside and outside of the fuel management area. The values of  $a_1$ ,  $a_4$ ,  $b_1$  and  $b_4$  that appear in the table are presented in real scale dimensions (scale factor equal to 1/16).

## Results.

As this is an ongoing work, we present here the preliminary results obtained in the described tests. The fire intensity of a fire front when the fire spread upslope and the temperature gradient in the face  $f_1$  of the infrastructure are presented. The ROS of the fire front is not presented because we consider the fire intensity is more relevant for problem. However, the fire intensity is directly related to the ROS, equation 11. The distances ( $Dis$ ) presented in **Figure 3** are related to the real distances, and for a better understanding of the reader we assign the name to the real scale dimensions.

In **Figure 3** the fire intensity when the fire spreads upslope is shown as a function of the distance travelled by the fire front. The lines *ref 2*, *ref 3*, and *ref 4* represent the mean values for each configuration presented in **Table 2** and the points represent the results for each test performed. The vertical dashed lines, *Start FM 50 meters* and *Start FM 25 meters*, correspond to the fuel load change from  $0.6$  to  $0.2 \text{ kg.m}^{-2}$ , that is the



beginning of the fuel management. These lines are associated to the tests performed with configurations of *ref 2* and *ref 3*. However, the line *ref 4* represent the configurations without fuel management surrounding the infrastructure. In the present analysis the fire intensity of tests with *ref 1* is not shown because those are equal to the tests *ref 2* but the fuel load inside of the fuel management is  $0 \text{ kg.m}^{-2}$ . For those tests (*ref 1*) the fire intensity near of the infrastructure is  $0 \text{ kW.m}^{-1}$ .

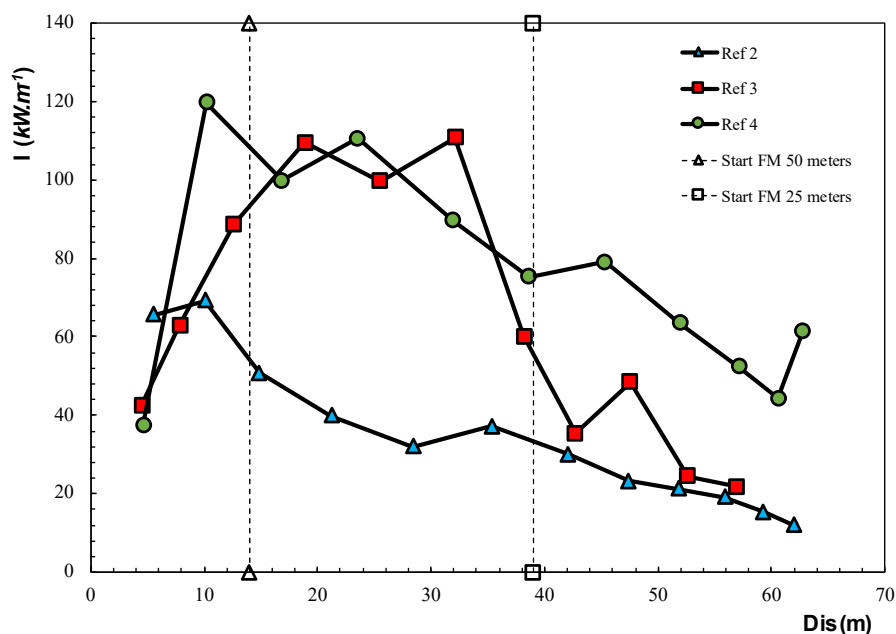


Figure 3. Fire intensity when the fire spreads upslope.

From these tests we may conclude that the fire intensity decreases significantly when the fuel load is reduced. Near the infrastructure, fire intensity obtained with tests *ref 4* showed values five times higher, compared to tests *ref 2* and *ref 3*. As previously shown, fire intensity and flame length are directly related. Flame length in areas without fuel management can be two times higher compared to where fuel management was made.

The fire intensity in tests *ref 2* increased normally but when the fire front reached the fuel management area the intensity of the fire decreased and, in these tests, the obtained results present lower intensity. The behaviour in tests *ref 3* is very identical to *ref 2* because during the beginning of the tests, when fuel load was  $0.6 \text{ kg.m}^{-2}$ , the fire intensity was equal to *ref 4* but during the approach and close to the infrastructure the intensity decreased to the same values of fire intensity in *ref 2*.

The temperature gradient of face  $f_1$  when the fire spread upslope is shown as a function of time, Figure 4. In this analysis the line *ref 1*, *ref 2*, *ref 3* and *ref 4* follows the same methodology of the previous results presented before (Figure 3) and represent the mean values for each test performed. The maximum temperature gradient happens when the fire front reached the infrastructure on the top of the slope and the interval time is approximately the same.

From these tests we may conclude that in tests without fuel management (*Ref 4*) the temperature gradient is higher ( $13.97 \text{ }^\circ\text{C.s}^{-1}$ ) compared to the test that had fuel management around the infrastructure (*Ref 2* =  $7.63 \text{ }^\circ\text{C.s}^{-1}$  and *Ref 3* =  $9.79 \text{ }^\circ\text{C.s}^{-1}$ ). When the fuel load around of the infrastructure is totally reduced (*Ref 1* -  $0 \text{ kg.m}^{-2}$ ) the values obtained are, during all the test time, approximately zero. It was also noticed that additional to the high values of temperature gradient, the duration time of this increment is more extended for the test *Ref 4* compared with the tests with fuel management *Ref 2*

and **Ref 3**. For the present study, we conclude that **Ref 1** corresponds to the best configuration because fire intensity in face  $f_1$  and the temperature gradient are approximately zero.

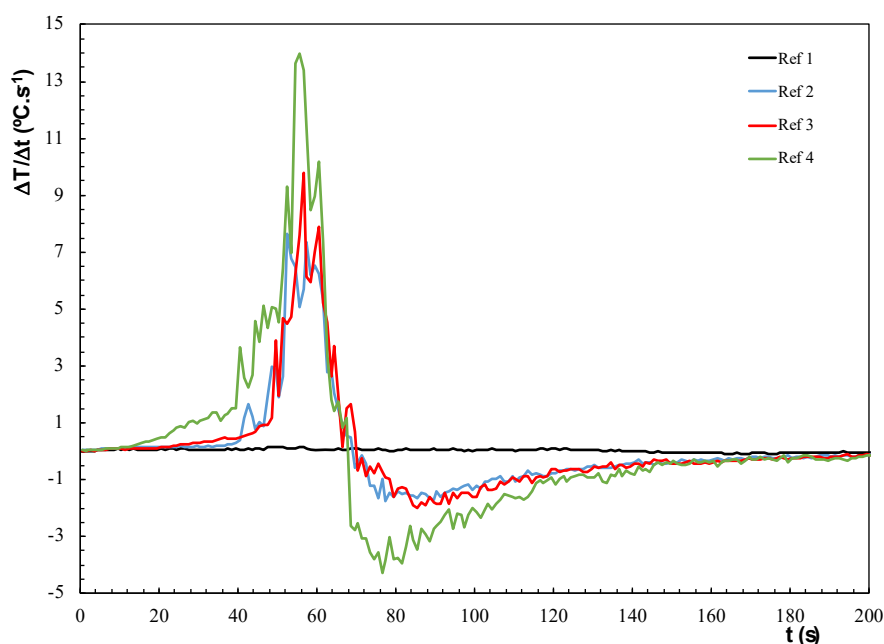


**Figure 4.** Temperature gradient in face  $f_1$  of infrastructure wall when the fire spread upslope.

When fuel management is done around the infrastructure and fuel load is reduced, the values of the temperature gradient in wall of the face  $f_1$  reduce in same way. In tests **Ref 3** the temperature gradient obtained is higher than in test **Ref 2**. This occurred in those tests not only because the fuel load is reduced (in both scenarios the fuel load is the same) but the distance of the fuel management in test **Ref 2** is higher than **Ref 3**. In this case the values of the fire intensity and the temperature gradient are directly correlated.

## Conclusions.

In the present study we tested a new methodology to assess the efficiency of fuel management surrounding isolated infrastructures, regarding fire impact. The tests were carried out at the Forest Fire Research Laboratory of University of Coimbra in Lousã on the Dihedral table. We performed tests with the fire spreading upslope and downslope. However, in these preliminary tests we only presented the results for upslope tests because the position of the infrastructure related to the infrared camera did not allow us to record the fire front in fuel management area. The results shown are only to the critical exposed face  $f_1$ . Three parameters were considered in those tests: the slope angle  $\alpha$ , the distance / area considered in the fuel management area and the variation of the fuel load outside and inside of the fuel management area.

The fuel management surrounding the infrastructures has a high importance in decreasing the risk or impact in infrastructures by a flaming front. The fire intensity when the fire spreads upslope without fuel management area is five times higher compared to when the tests were performed with fuel management area. Flame length is two times higher for the same conditions. This relation is independent of the distance of

fuel management. In the tests with 50 linear meters of fuel management, fire intensity presents the lower values of all.

The temperature gradient in this study is higher when the fuel management around the infrastructure is not made. However, it was also noticed that additional to the high values of temperature gradient the duration time of this increment is more extended for the test without fuel management. For the present study, we conclude that tests *Ref 1* is the best configuration because the fire intensity in face  $f_I$  and the temperature gradient are approximately zero.

The present work is the preliminary analysis of a new methodology to assess the efficiency of fuel management surrounding isolated infrastructures. We conclude that this methodology, in laboratory tests, presents the results expected for this configuration. However, for a better validation more research has to be carried to explore other experimental configurations in laboratory and in the field. In future work we intend to change the fuel type, the fuel load inside and outside of fuel management area and the slope angles when the fire spreads upslope or downslope.

### **Funding.**

This work was supported by project WUIVIEW - Wildland-Urban Interface Virtual Essays Workbench. with the Ref. ECHO/2018/826522, financed by EU Civil Protection Mechanism and by the project “ReNATURE - Valorisation of the Natural Endogenous Resources of the Centro Region” (Centro 2020, Centro-01-0145-FEDER-000007) supported by European Investment Funds by FEDER.

We would like to thank the FCT-Foundation for Science and Technology for the Ph.D. grants of Carlos Ribeiro with the reference SFRH/BD/140923/2018 and André Rodrigues with the reference SFRH/BD/138235/2018.

### **Acknowledgments.**

We would like to express our gratitude to Gonçalo Rosa for his support in laboratory tests.

**Bibliography.**

- Abrams JB, Knapp M, Paveglio TB, Ellison A, Moseley C, Nielsen-Pincus M, Carroll MS (2014) Re-envisioning community-wildfire relations in the U . S . West as adaptive. *Ecology and Society* **20**, 1–27. doi:Artn 34 10.5751/Es-07848-200334.
- Alcasena FJ, Ager AA, Bailey JD, Pineda N, Vega-García C (2019) Towards a comprehensive wildfire management strategy for Mediterranean areas: Framework development and implementation in Catalonia, Spain. *Journal of Environmental Management* **231**, 303–320. doi:10.1016/j.jenvman.2018.10.027.
- Barrera-Escoda (2011) Climate change projections for Catalonia (NE Iberian Peninsula). Part I: Regional climate modeling. *Tethys, Journal of Weather and Climate of the Western Mediterranean* 75–87. doi:10.3369/tethys.2011.8.08.
- Byram G (1959) Combustion of Forest Fuels. 'Ecology'. pp. 609–610. doi:10.2307/1932261.
- Cardil A, Delogu GM, Molina-Terrén DM (2017) Fatalities in Wildland Fires From 1945 To 2015 in Sardinia (Italy). *Cerne* **23**, 175–184. doi:10.1590/01047760201723022266.
- Cardil A, Molina DM, Kobziar LN (2014) Extreme temperature days and their potential impacts on southern Europe. *Natural Hazards and Earth System Sciences* **14**, 3005–3014. doi:10.5194/nhess-14-3005-2014.
- Costa P, Castellnou M, Larrañaga A, Miralles M, Kraus D (2011) 'Prevention of Large Wildfires using the fire types concept.' doi:10.1080/10910340802067536.
- Manzello SL, Suzuki S, Hayashi Y (2012) Enabling the study of structure vulnerabilities to ignition from wind driven firebrand showers: A summary of experimental results. *Fire Safety Journal* **54**, 181–196. doi:10.1016/j.firesaf.2012.06.012.
- Moreira F, Viedma O, Arianoutsou M, Curt T, Koutsias N, Rigolot E, Barbati A, Corona P, Vaz P, Xanthopoulos G, Mouillot F, Bilgili E (2011) Landscape - wildfire interactions in southern Europe: Implications for landscape management. *Journal of Environmental Management* **92**, 2389–2402. doi:10.1016/j.jenvman.2011.06.028.
- Pyne SJ, Andrews PL, Laven RD (1996) 'Introduction to wildland fire.' (John Wiley and Sons: New York)
- Rothermel RC, Deeming JE (1980) Measuring and interpreting fire behavior for correlation with fire effects. *General Technical Report INT-93*, 6.
- Valente S, Coelho C, Ribeiro C, Liniger H, Schwilch G, Figueiredo E, Bachmann F (2015) How much management is enough? Stakeholder views on forest management in fire-prone areas in central Portugal. *Forest Policy and Economics* **53**, 1–11. doi:10.1016/j.forpol.2015.01.003.
- Viegas DX (2005) A Mathematical Model For Forest Fires Blowup. *Combustion Science and Technology* **177**, 27–51. doi:10.1080/00102200590883624.
- Viegas DX, Almeida M, Ribeiro L, Raposo J, Viegas MT, Oliveira R, Alves D, Pinto C, Humberto J, Rodrigues A, Lucas D, Lopes S, Silva L (2017) O COMPLEXO DE INCÊNDIOS DE PEDRÓGÃO GRANDE E CONCELHOS LIMÍTROFES, INICIADO A 17 DE JUNHO DE 2017. (Coimbra, Portugal)